IOPscience iopscience.iop.org

Home Search Collections Journals About Contact us My IOPscience

Light scattering cross section from surface acoustic phonons in multilayer films

This article has been downloaded from IOPscience. Please scroll down to see the full text article.

1993 J. Phys.: Condens. Matter 5 7353

(http://iopscience.iop.org/0953-8984/5/40/010)

View the table of contents for this issue, or go to the journal homepage for more

Download details:
IP Address: 171.66.16.96
The article was downloaded on 11/05/2010 at 01:56

Please note that terms and conditions apply.

J. Phys.: Condens. Matter 5 (1993) 7353–7360. Printed in the UK

Light scattering cross section from surface acoustic phonons in multilayer films

F Nizzoli, O Donzelli and C Arcangeli

Dipartimento di Fisica, Università di Ferrara, Via Paradiso, 12-44100 Ferrara, Italy and Consorzio Interuniversitario Nazionale Fisica della Materia, Italy

Received 20 July 1993

Abstract. We calculate the Brillouin cross section from surface and guided acoustic modes in opaque multilayer supported films by including the ripple scattering at all the interfaces. The results are compared with the usual approximate calculations. The superlattices Ag/Pd and Mo/Si are studied. We investigate in detail the dependence of the cross section on the top layer and the limit of validity of the effective-medium approximation. It is found that this approximation is no longer valid in case of a long-period metal–semiconductor superlattice such as Mo/Si.

The theory of Brillouin scattering (BS) by surface and guided acoustic waves was developed a few years ago for supported [1] and free-standing films [2,3]. The theory has been more recently extended to a metal–dielectric bilayer deposited onto a prism, in order to study surface-polariton-enhanced BS [4]. It is well known that, in general, two mechanisms contribute to the scattering cross section in a film: the elasto-optic coupling between the light and the elastic waves and the inelastic scattering of the electromagnetic radiation by the dynamical corrugations produced at each interface by the surface waves (ripple mechanism).

BS has been also widely used in the last decade to investigate the elastic properties of metal superlattices [5]. The first comparison between measured and calculated BS spectra of a metal superlattice (Mo/Ta) has been published by Bell *et al* [6]. In that paper the calculations were based on the assumption that the Brillouin cross section of a multilayer metal film is completely dominated by the ripple mechanism at the film free surface, in analogy with the case of a semi-infinite metallic medium [7]; we will call this approximation the surface-ripple approximation (SRA). In a superlattice, however, if one neglects the elasto-optic coupling, as seems justified in metals, the ripple scattering occurs, at least in principle, at all the interfaces. Therefore the scattered electromagnetic field contains several contributions, with possible interference effects between them. It is known that in a supported transparent film such effects are very large [8].

The comparison between theory (SRA) and experiment in the above-mentioned case [6] turned out to be extremely good: the relative amplitudes of the experimental peaks due to the surface and guided modes in the multilayer supported film were reproduced by the theory with high accuracy. The same assumption (SRA) has been used later, and successfully, by Dutcher *et al* [9] in order to assign the structures of the BS spectra of Ag/Pd superlattices due to the Rayleigh wave (RW), to the Sezawa waves and to the longitudinal guided modes [10].

It should be noted that in the previous cases [6, 9] the comparison between theory and experiment was limited to the relative amplitudes of the various structures of a single BS spectrum, the absolute intensities having not been considered. For example, no investigation

0953-8984/93/407353+08$07.50 © 1993 IOP Publishing Ltd

of the dependence of the cross section on the properties of the outermost layer has been carried out. In the present paper we address calculations of the BS cross section of strongly absorbing multilayers (metal–metal and metal–semiconductor periodic superlattices) by including ripple scattering at all the interfaces between the two media. Our aims are: to verify the conditions of validity of the SRA and of the effective-medium approximation in the theory of the BS cross section and to study the dependence of the calculated BS cross section of superlattices on the different approximations and on the surface layer.

It is well known from the theory of elasticity [11] that the long-wavelength elastic properties of an ideal layered medium can be expressed in terms of effective elastic constants, provided that the excitation wavelength is longer than the modulation wavelength of the superlattice $\Lambda = d_A + d_B$, where d_A and d_B are the thicknesses of the layers A and B respectively. Recently general expressions have been derived that allow us to calculate explicitly the effective elastic constants of a superlattice in the long-wavelength limit as a function of the bulk elastic constants of the two components and of the thickness ratio d_A/d_B [12]. It is also known that several metal superlattices show elastic anomalies in the range $\Lambda = 20$–80 Å, i.e. the effective elastic constants depend on Λ and differ from those calculated from the bulk values [5]. However in the present paper we are not interested in this problem. A general approach for the calculation of elementary excitations in arbitrary continuous superlattices by explicitly considering the effects of the interfaces can be found in [13]. In the following we assume the validity of the effective-medium approximation for the calculation of the velocity and of the displacement field of the surface and guided waves in a supported multilayer film. In contrast we focus our attention on the cross-section effects and we present an exact treatment of the interaction of light with the surface acoustic phonons in a superlattice, by explicitly considering the stratified nature of this medium, in other words by taking into account the ripple scattering at each interface.

We consider acoustic modes polarized in the sagittal plane, such as the Rayleigh surface wave and the Sezawa guided waves. The incident and scattered light beams are p polarized, i.e. the magnetic field $\boldsymbol{B}$ is perpendicular to the scattering (sagittal) plane. We assume a back-scattering geometry, with θ as incidence and scattering angle, calculated with respect to the surface normal. In this framework the Brillouin differential cross section for a given phonon mode of frequency Ω and parallel wavevector Q is given by [14]

$$d^2\sigma/d\Omega_a\, d\omega \propto \cos\theta\,(|B_S(\Omega)/B_0|^2)\delta(\Omega - |\omega - \omega_0|) \tag{1}$$

where the incoming light has frequency ω_0 and magnetic field amplitude B_0 and the back-scattered light in vacuum has frequency ω and magnetic field amplitude $B_S(\Omega)$. Ω_a is the solid angle. The brackets indicate the thermal average.

The scattered field $B_S(\Omega)$ can be calculated by imposing the electromagnetic boundary conditions at each interface, i.e. the continuity of B and of the tangential component of the electric field, i.e. $(\epsilon^{-1}\nabla \times \boldsymbol{B})_t$, on the N phonon corrugated interfaces. To zero order in the phonon displacement field, the interfaces are flat and one easily obtains the Fresnel expressions for the transmitted and reflected field B. When the dynamical corrugations at each interface are taken into account, the boundary conditions can be written to first order in the shear vertical component $U_z(z, \Omega, Q)$ of the phonon field [1, 4, 14]. The coordinate normal to the surface is labelled by z. Finally a linear inhomogeneous system of $2N$ equations is obtained, having as unknowns the amplitudes of the transmitted and reflected scattered magnetic field $B(\Omega)$ in each layer and in vacuum. This system can be numerically solved and in particular the back-scattered field in vacuum $B_S(\Omega)$ can be evaluated in terms

of U_z. Therefore the thermal average term in equation (1) can be written in the form

$$\left\langle \left| \frac{B_S(\Omega)}{B_0} \right|^2 \right\rangle = \sum_{i=1}^{N} \left| C_i \frac{U_z(z_i, \Omega, Q)}{\Omega} \right|^2 \tag{2}$$

where the index i labels the superlattice interfaces located at the depths z_i and the coefficients C_i depend on the dielectric constants of the media and on the structure of the superlattice. For a supported layer [1] or a bilayer [4] these coefficients have been calculated analytically; in a superlattice with $N \gg 3$ they can be either calculated with the transfer-matrix technique [15] or evaluated numerically by solving a large linear system of equations. In the following we present for two multilayer systems our results obtained with the latter technique.

We study the BS cross section of the Ag/Pd superlattice deposited on sapphire, which has already been investigated experimentally [9], and of the Mo/Si superlattice grown on (001) Si, as representative of metal–semiconductor systems used in x-ray optics [16]. We neglect the elasto-optic contribution to the cross section also in the case of Mo/Si because it is known that in Si, as in metals, the Brillouin spectra from surface excitations are dominated by the ripple effect [17]. In this paper we are not interested in bulk phonon features, which in contrast in Si would necessarily require the inclusion of the elasto-optic coupling. The effective elastic properties of these systems, used to calculate the surface phonons and their displacement fields, are given in table 1. Both films are modelled as hexagonal media with the c axis perpendicular to the substrate surface. The substrates are assumed to be cubic, bounded by the (001) surface, and the phonon propagation direction is along [100]. The data for Ag/Pd on sapphire, taken from [9], represent a best fit to BS spectra. The data for Mo/Si are calculated effective elastic constants of a multilayer composed of amorphous Si and polycrystalline Mo (Voigt average). Table 2 shows the thickness of the layers and their dielectric properties. The wavelength of the incident light is $\lambda = 5145$ Å.

Table 1. Data for multilayer films and substrates used in the calculation of the displacement field. The elastic constants c_{ij} are given in GPa. The density ρ in g cm^{-3}, the total film thickness h in Å and the scattering angle θ in degrees.

Medium	c_{11}	c_{13}	c_{33}	c_{55}	ρ	h	θ
Ag/Pd	193	119	195	32.3	11.23	4570	70
Sapphire	497	203	497	147	3.986	—	—
Mo/Si	297	93.8	263	87.7	6.265	8000	70
Si	166	63.9	166	79.6	2.33	—	—

Table 2. Real (ϵ_1) and imaginary part (ϵ_2) of the dielectric function of the multilayer components used in the calculations. The thickness d of each layer is given in Å.

Layer	ϵ_1	ϵ_2	d
Ag	−10.7	0.327	18.5
Pd	−10.8	11.40	18.5
Mo	−1.40	27.14	200
Si	18.5	0.52	200

Figure 1 shows the calculated cross section for three selected acoustic modes of the Ag/Pd superlattice on sapphire, as a function of the number N of interfaces included in the calculation (the sum appearing in equation (2)). It can be seen that for the first two modes the sum converges by including about 30 layers, corresponding to a film depth of 555 Å. The convergence is even faster for the third mode because its decay constant in the film is larger. The following conclusions can be drawn: (a) contrary to the commonly accepted belief the ripple contributions from the buried interfaces are large and the interference effects remarkable; (b) the exact values ($N \to \infty$) are about 20% larger than the surface values (SRA); and (c) although the absolute values of the cross section oscillate strongly in figure 1 for the first 15 layers, the relative amplitudes of the cross section for the different phonon modes remain almost unchanged during the iteration procedure. The reason is that for small modulation wavelengths (Λ much less than the typical oscillation periods of $U_z(z, \Omega, Q)$) the displacement fields are almost constant across each AB bilayer, giving rise to a fine cancellation between the ripple contributions of two contiguous interfaces.

In figure 2 a similar analysis is carried out for the RW (mode 1) of the same superlattice, but with Pd as top layer. Although the cross section due to the first interface (metal–vacuum) depends strongly on the top medium, the exact asymptotic values are almost identical. In table 3 a comparison between absolute values of the cross section for the RW is shown. As already remarked, for this superlattice the exact values (last two columns) do not depend appreciably on the top layer and a good approximation is obtained by modelling the superlattice as a single film with an effective dielectric constant of hexagonal symmetry ϵ_{eff} [15]. This means that the effective-medium approximation works well in Ag/Pd, as far as the calculation of the light cross section is concerned. The effective dielectric tensor for Ag/Pd is given by: $\epsilon_{xx} = -10.7 + 5.86\text{i}$; $\epsilon_{zz} = -12.9 + 4.63\text{i}$. Finally figure 3 presents the comparison between the calculated and the experimental BS data for this superlattice: it turns out that the agreement is very good. In this figure a single calculated curve has been shown because the SRA and the full theory give the same spectrum, apart from a scale factor. On the other hand, to the best of our knowledge, an absolute comparison between experimental and calculated BS spectra is not possible because of large indeterminations in the measured intensity.

Table 3. Values of the Brillouin cross section of the RW for the Ag/Pd and Mo/Si superlattices, according to different models. The first three columns refer to calculations in the SRA, assuming as dielectric constant of the whole film that of the material A, of the material B and of the effective-medium respectively. The last two columns refer to the exact calculations where ripple scattering from all the interfaces is included: the two values depend on the top layer (A or B).

	Calculated cross section (in arbitrary units)				
Multilayer	$\epsilon(A)$	$\epsilon(B)$	ϵ_{eff}	Top layer: A	Top layer: B
Ag(A)/Pd(B)	1.604	1.066	1.144	1.182	1.125
Mo(A)/Si(B)	3.060	1.491	1.607	3.263	0.124

In the case of the Mo/Si multilayer, we have chosen a modulation wavelength Λ = 400 Å, larger than in the previous superlattice. Also the optical contrast is much larger. As a matter of fact the results are quite different form those of Ag/Pd, as can be seen in table 3. The effective-medium approximation for the cross section is no longer valid and the top layer plays an essential role. Even more striking is the different behaviour of the cross section of the different phonon modes when the top layer is Si. In figure 4 it is shown that two modes

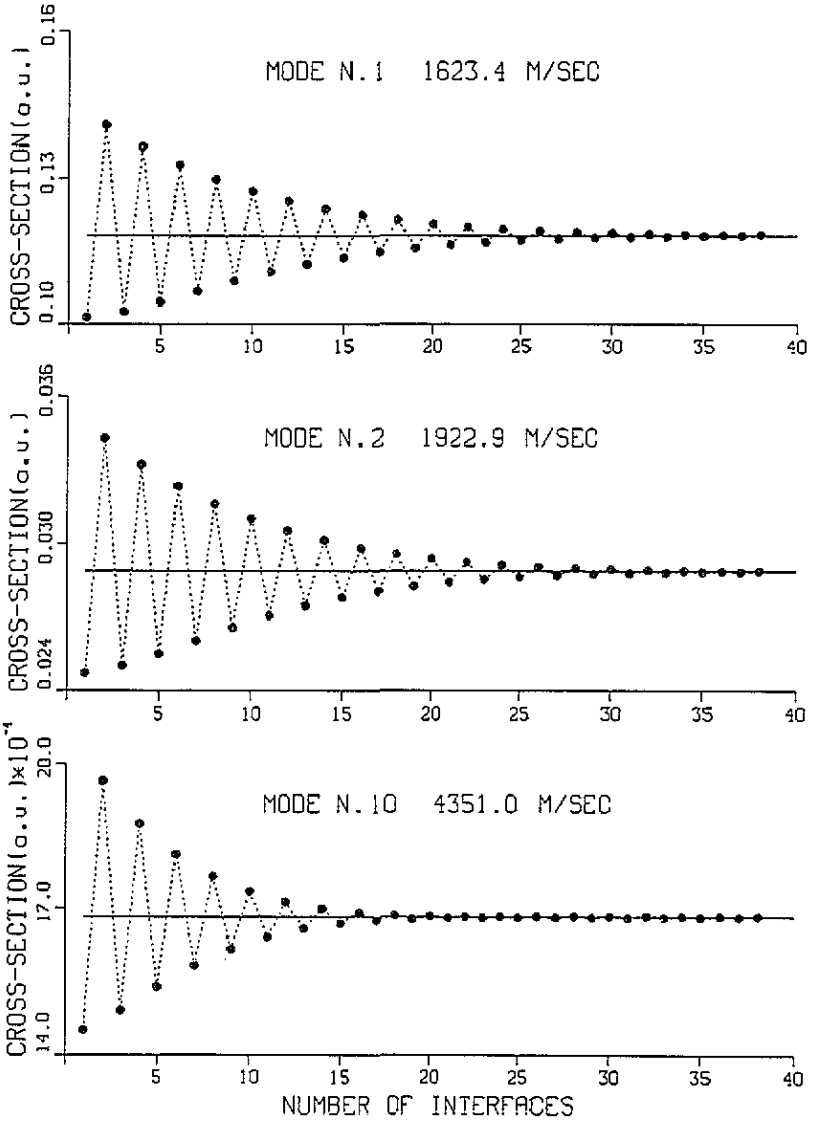

Figure 1. Brillouin cross section for three modes, as a function of the number of interfaces included in the calculation, for the Ag/Pd superlattice. The propagation velocity of each mode is also indicated. The top layer is Ag. Mode N. 1: surface wave (RW). Mode N. 2: first-order Sezawa wave. Mode N. 10: longitudinal guided wave. The dotted lines are guides for the eyes.

(the RW and the sixth-order Sezawa mode) are affected differently by the inclusion in the sum of equation (2) of the first five relevant terms, needed to reach convergence. This is actually due to the strong optical contrast and to the large modulation wavelength, as in the four top layers the displacement field of the RW is almost constant while the displacement field of the Sezawa mode decreases to zero and even changes its sign. This is illustrated in figure 5. Finally the exact cross section and the approximated one (SRA) are compared in figure 6. The amplitude of the Sezawa peaks, with respect to the RW peak, is strongly

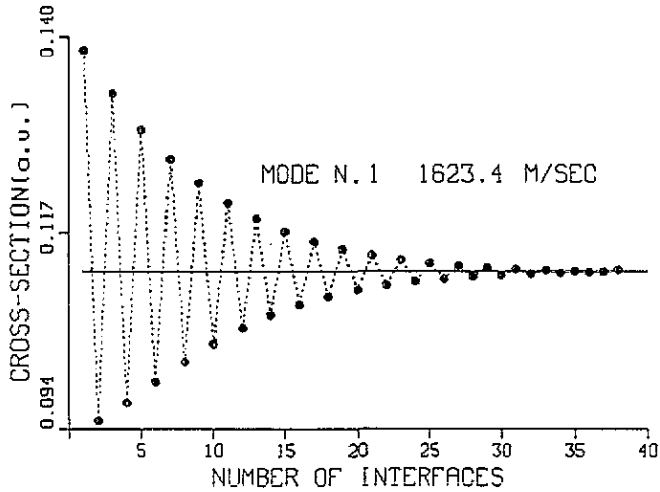

Figure 2. Brillouin cross section for the surface mode (RW), as a function of the number of interfaces included in the calculation, for the Ag/Pd superlattice. The top layer is Pd.

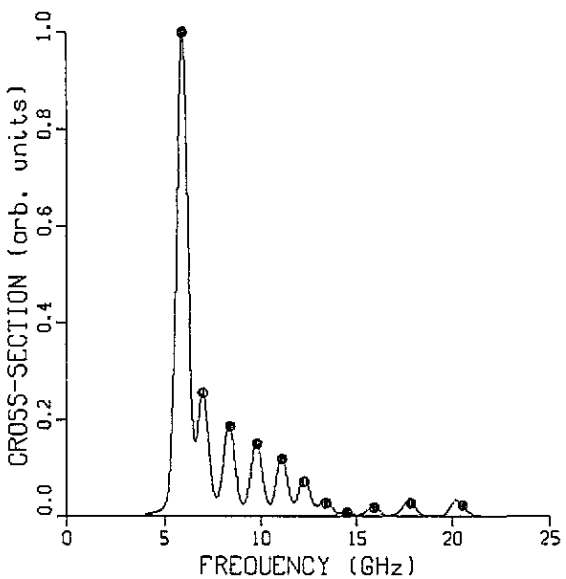

Figure 3. Calculated Brillouin cross section (full curve) compared with the experimental data, taken from [9]. The filled circles represent the frequencies and the intensities of the experimental peaks. Theoretical and experimental curves are normalized in such a way as to show the same amplitude for the lowest frequency mode (RW).

affected by the inclusion of ripple scattering by the four interfaces immediately underneath the film free surface. Note that in this particular case an enhancement of the peak intensity in the guided-mode frequency range is predicted by the full theory with respect to the SRA.

In summary, we have calculated for the first time the light cross section in opaque superlattices by including the ripple scattering from all the interfaces. In general we have found that the ripple contributions from the interfaces underneath the film surface are large. However the net result of the inclusion of these effects depends on the physical properties of the system under consideration.

Two limiting cases have been investigated in detail. In a metal–metal superlattice with

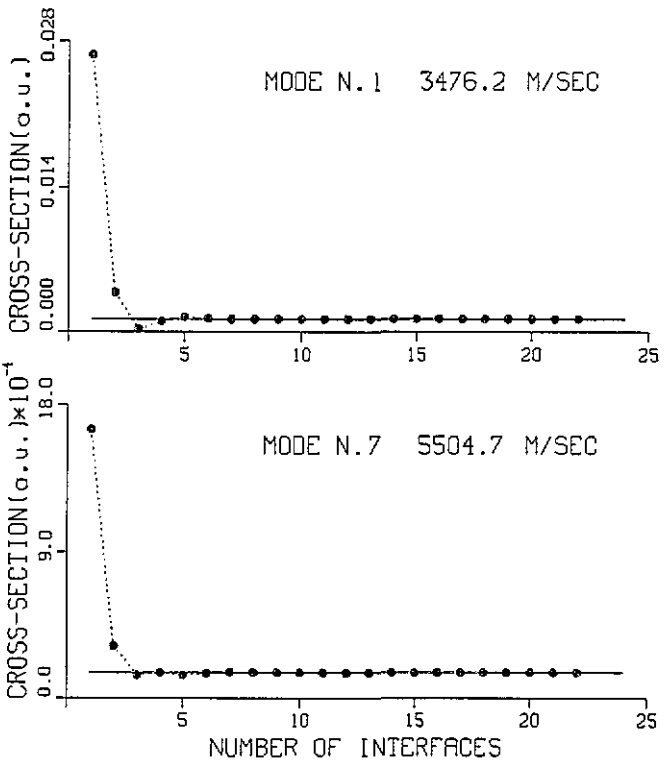

Figure 4. Brillouin cross section for two modes, as a function of the number of interfaces included in the calculation, for the Mo/Si superlattice. The top layer is Si. Mode N. 1: surface wave (RW). Mode N. 7: sixth-order Sezawa wave.

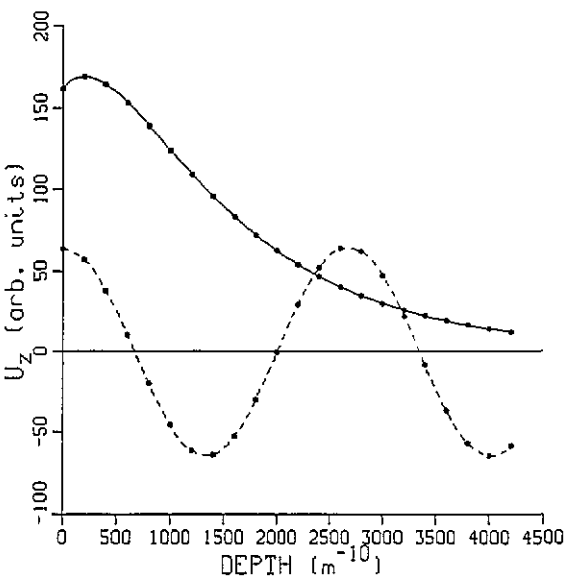

Figure 5. Shear vertical displacement component $U_z(z, \Omega, Q)$ versus the depth z, measured from the film free surface, in the Mo/Si superlattice: full curve, RW; broken curve, sixth-order Sezawa wave (these two modes are the same as those considered in figure 4). The dots mark the interfaces.

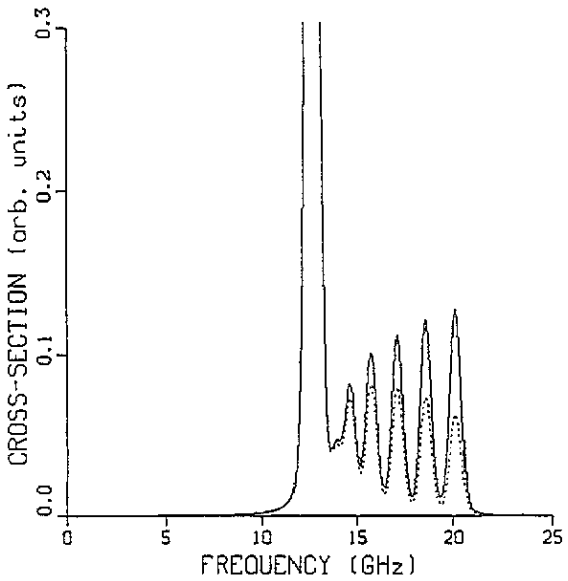

Figure 6. Calculated cross section for the Mo/Si superlattice. The top layer is Si. Full curve, exact calculation including ripple scattering at all the interfaces; dotted curve, SRA. The two curves are normalized in such a way that the amplitude of the lowest frequency peak is the same in the two cases.

small modulation wavelength ($\Lambda = 37$ Å) and a relatively small optical contrast between the two media (as in Ag/Pd) the SRA accurately reproduces the relative strength of the cross section for the different phonon modes. Even the absolute value of the cross section can be calculated with good accuracy in the effective-medium approximation. In contrast in a metal–semiconductor multilayer (such as Mo/Si) with large modulation wavelength ($\Lambda = 400$ Å) the shape of the BS spectra is affected by the ripple scattering from the buried interfaces and the amount of scattered light depends on the top layer, so that the effective-medium approximation loses its validity.

This work was partially supported by Ministero Università e Ricerca Scientifica e Tecnologica.

References

[1] Bortolani V, Marvin A, Nizzoli F and Santoro G 1983 *J. Phys. C: Solid State Phys.* **16** 1757
[2] Albuquerque E L, Loudon R and Tilley D R 1980 *J. Phys. C: Solid State Phys.* **13** 1775
[3] Albuquerque E L, Oliveros M C and Tilley D R 1984 *J. Phys. C: Solid State Phys.* **17** 1451
[4] Marucci N and Nizzoli F 1990 *Surf. Sci.* **236** 175
[5] Grimsditch M 1989 *Topics in Applied Physics* vol 66, ed M Cardona and G Güntherodt (Berlin: Springer) p 283
[6] Bell J A, Bennet W R, Zanoni R, Stegeman G I, Falco C M and Nizzoli F 1987 *Phys. Rev.* B **35** 4127
[7] Loudon R 1978 *Phys. Rev. Lett.* 40 581
[8] Bortolani V, Santoro G, Nizzoli F and Sandercock J R 1982 *Phys. Rev.* B **25** 3442
[9] Dutcher J R, Lee S, Kim J, Stegeman G I and Falco C M 1988 *Phys. Rev. Lett.* **65** 1231
[10] Hillebrands B, Lee S, Stegeman G I, Cheng H, Potts J E and Nizzoli F 1988 *Phys. Rev. Lett.* **60** 832
[11] Bruggeman D A G 1937 *Ann. Phys., Lpz.* **29** 160
[12] Grimsditch M and Nizzoli F 1986 *Phys. Rev.* B **33** 5891
[13] Garcia Moliner F and Velasco V R 1986 *Surf. Sci.* **175** 9
[14] Marvin A, Bortolani V and Nizzoli F 1980 *J. Phys. C: Solid State Phys.* **13** 299
[15] Sapriel J and Djafari Rouhani D 1989 *Surf. Sci. Rep.* **10** 189
[16] Slaughter J M, Shapiro A, Kearney P A and Falco C M 1991 *Phys. Rev.* B **44** 3854
[17] Marvin A, Bortolani V, Nizzoli F and Santoro G 1980 *J. Phys. C: Solid State Phys.* **13** 1607